

Influence of incommensurate dynamic charge-density wave scattering on the line shape of superconducting high- T_c cuprates

G. Seibold[†] and M. Grilli^{*}

[†] Institut für Physik, BTU Cottbus, PBox 101344, 03013 Cottbus, Germany

^{*} Istituto Nazionale di Fisica della Materia e Dipartimento di Fisica, Università di Roma “La Sapienza”, Piazzale A. Moro 2, 00185 Roma, Italy

We show that the spectral lineshape of superconducting $\text{La}_{2-x}\text{Sr}_x\text{CuO}_4$ (LSCO) and $\text{Bi}_2\text{Sr}_2\text{CaCu}_2\text{O}_{8+\delta}$ (Bi2212) can be well described by the coupling of the charge carriers to collective incommensurate charge-density wave (CDW) excitations. Our results imply that besides antiferromagnetic (AF) fluctuations also low-energy CDW modes can contribute to the observed dip-hump structure in the Bi2212 photoemission spectra. In case of underdoped LSCO we propose a possible interpretation of ARPES data in terms of a grid pattern of fluctuating stripes where the charge and spin scattering directions deviate by $\alpha = \pi/4$. Within this scenario we find that the spectral intensity along $(0, 0) \rightarrow (\pi, \pi)$ is strongly suppressed consistent with recent photoemission experiments. In addition the incommensurate charge-density wave scattering leads to a significant broadening of the quasiparticle-peak around $(\pi, 0)$.

I. INTRODUCTION

The proximity to a charge density instability tuned by doping and temperature allows to interpret many properties of the cuprates in the framework of a Quantum Critical Point (QCP) physics [1,2] located near optimal doping [3–5]. Within this scenario the singular scattering induced by the critical charge fluctuations would be responsible for both the anomalous normal-state properties and the large superconducting critical temperatures. Then the phase diagram of the cuprates is partitioned in a (nearly) ordered, a quantum critical, and a quantum disordered region naturally corresponding to the under-, optimally, and over-doped regions of the phase diagram of the cuprates respectively.

First evidence for incommensurate stripe structures in the high- T_c compounds was given by neutron scattering experiments [6] in Nd-doped lanthanum cuprate where due to distortions of the LTT lattice both magnetic and charge-order peaks where detectable. However, also in Nd-free materials including the YBCO compounds where only the magnetic incommensurate peak has been observed [7,8] the simultaneous occurrence of charge order has been claimed by NQR measurements [9–11]. Moreover, it has been argued [12] that the QCP can be deduced from the incommensurate neutron peak intensity which vanishes in the slightly overdoped regime $x \approx 0.19$. This coincides surprisingly well with experiments in $\text{La}_{2-x}\text{Sr}_x\text{CuO}_4$ (LSCO) compounds where superconductivity has been suppressed by pulsed magnetic fields [13] showing an underlying metal-insulator transition at about the same critical doping.

The strong charge-density wave (CDW) scattering should have strong effects on the electronic self-energy Σ which one in principle can extract from angle-resolved photoemission (ARPES) data. In the $\text{Bi}_2\text{Sr}_2\text{CaCu}_2\text{O}_{8+\delta}$ (Bi2212) compounds these spectra are characterized by

an unusual lineshape around $(\pi, 0)$ which consists of a sharp peak at low energy followed by a hump at higher energies. Both features are separated by a dip. In addition the sharp peak persists at low energy over a large region in k -space whereas the hump correlates well with the underlying normal state dispersion [14]. It has been shown in Ref. [15] that these features can be well described by assuming that the electrons are coupled to a dispersionless collective mode. Moreover, since the dispersions around $(\pi, 0)$ along the two orthogonal directions $M \rightarrow \Gamma$ and $M \rightarrow Y$ are similar it was suggested [16] that the (π, π) collective mode, observed in inelastic neutron scattering, is intimately connected with the mechanism leading to superconductivity.

Recent photoemission experiments [17] on superconducting underdoped $\text{La}_{2-x}\text{Sr}_x\text{CuO}_4$ (LSCO) have also revealed a broad quasiparticle peak (QP) around the $(\pi, 0)$ point. On the other hand no QP can be identified along the $(0, 0) \rightarrow (\pi, \pi)$ direction in contrast to the Bi2212 compound where along the diagonals a clear Fermi surface crossing has been observed. Exact diagonalization studies of the $t-t'-t''-J$ model with an additional phenomenological stripe potential [18] have demonstrated that these features may be due to the coupling of the holes to vertical charged (static) stripes.

In the present paper we want to focus on the dynamic aspect of incommensurate CDW scattering within the framework of a Quantum Critical Point (QCP) scenario. In this context we discuss the differences between the photoemission spectra of Bi2212 and LSCO respectively. Especially we show that the different features can be explained by the assumption that in Bi2212 the charge carriers couple to an incommensurate CDW oriented along the $(1, 0)-$ and $(0, 1)-$ directions whereas in LSCO the dynamic CDW scattering is along the diagonals. The results presented below supplement considerations of Ref. [19] where we have shown that a two-

dimensional 'eggbox-type' charge-pattern can reproduce the essential features of the normal state Bi2212 Fermi surface, namely the reduction of spectral weight around the M-points associated with the opening of a pseudo-gap in these regions of k-space. Here we extend our considerations to the case of LSCO assuming that the k-dependence of the electron self-energy is an essential ingredient in the description of ARPES data.

After having introduced the formalism in Sec. II we will present in Sec. III the analysis of ARPES spectra for both LSCO and Bi2212 materials. We finally conclude our discussion in Sec. IV.

II. FORMALISM

We consider a system of superconducting electrons exposed to an effective action

$$S = -\lambda^2 \sum_q \int_0^\beta d\tau_1 \int_0^\beta d\tau_2 \chi_q(\tau_1 - \tau_2) \rho_q(\tau_1) \rho_{-q}(\tau_2) \quad (1)$$

describing dynamical incommensurate CDW fluctuations. Using Nambu-Gorkov notation the unperturbed Matsubara Greens function matrix $\underline{\underline{G}}$ is given by

$$\begin{aligned} G_{11}^0(k, i\omega) &= \frac{u_k^2}{i\omega - E_k} + \frac{v_k^2}{i\omega + E_k} \\ G_{22}^0(k, i\omega) &= \frac{v_k^2}{i\omega - E_k} + \frac{u_k^2}{i\omega + E_k} \\ G_{12}^0(k, i\omega) &= G_{21}^0(k, i\omega) = -u_k v_k \left[\frac{1}{i\omega - E_k} - \frac{1}{i\omega + E_k} \right] \end{aligned} \quad (2)$$

where the BCS coherence factors are defined as $u_k^2 = \frac{1}{2}(1 + \frac{\epsilon_k - \mu}{E_k})$ and $v_k^2 = \frac{1}{2}(1 + \frac{\epsilon_k + \mu}{E_k})$ respectively. The leading order one-loop contribution to the self-energy reads as

$$\underline{\underline{\Sigma}}(k(i, \omega)) = -\frac{\lambda^2}{\beta} \sum_{q, ip} \chi_q(ip) \underline{\underline{G}}^0(k - q, i\omega - ip) \quad (5)$$

which in turn allows for the calculation of $\underline{\underline{G}}$ via

$$\underline{\underline{G}} = \underline{\underline{G}}^0 + \underline{\underline{G}}^0 \underline{\underline{\Sigma}} \underline{\underline{G}}. \quad (6)$$

Finally the spectral function can be extracted from $A_k(\omega) = \text{Im}G_{11}(k, \omega)$.

Note that our approach differs from the standard Elisahberg treatment by the fact that already the unperturbed system displays coherent superconducting order. Since the incommensurate CDW fluctuations have been shown to be strongly attractive in the d-wave channel [4] the idea is to incorporate this feature already on the zeroth order level by a frequency independent d-wave order parameter. Thus the self-energy is gapped by $\underline{\underline{G}}^0$, however, for our present considerations this approximation is sufficient since we are interested in line shape phenomena occurring at energies $\omega \gg \Delta^{SC}$.

III. RESULTS

In order to simplify the calculations we consider a Kampf-Schrieffer-type model susceptibility [20] which is factorized into an ω - and q -dependent part, i.e.

$$\chi_q(\omega) = W(\omega) J(\mathbf{q}) \quad (7)$$

where $W(\omega) = -\int d\nu g(\nu) 2\nu/(\omega^2 + \nu^2)$ is some distribution of dispersionless propagating bosons and

$$J(\mathbf{q}) = \frac{1}{4} \sum_{\pm q_x^c; \pm q_y^c} \frac{\Gamma}{\Gamma^2 + 2 - \cos(q_x - q_x^c) - \cos(q_y - q_y^c)} \quad (8)$$

contains the charge-charge correlations which are enhanced at the four equivalent critical wave vectors $(\pm q_x^c, \pm q_y^c)$. As we will show below the static limit $g(\nu) = \delta(\nu)$ with infinite charge-charge correlation length $\Gamma \rightarrow 0$ allows one to relate the coupling parameter λ to the parameter set of the Hubbard-Holstein model with long-range Coulomb interaction by following the approach in Ref. [19]. Concerning the normal state dispersion we use a tight-binding fit to normal state ARPES data [21,22] including the hopping between first, second and third nearest neighbors, i.e. $\epsilon_k = t(\cos(k_x) + \cos(k_y))/2 + t' \cos(k_x) \cos(k_y) + t''(\cos(2k_x) + \cos(2k_y))/2$. (3) (4) For Bi2212 we take $t = -0.59$, $t' = 0.164$, $t'' = -0.052$ and for LSCO $t = -0.35$, $t' = 0.042$, $t'' = -0.028$. The BCS gap is assumed to be d-wave symmetry $\Delta_{SC}(\mathbf{k}) = \Delta_0(\cos(k_x) - \cos(k_y))$ where $\Delta_0(\text{Bi2212}) = 32\text{meV}$ and $\Delta_0(\text{LSCO}) = 10\text{meV}$ respectively.

A. $\text{Bi}_2\text{Sr}_2\text{CaCu}_2\text{O}_{8+\delta}$

In Ref. [19] we have already demonstrated that a static two-dimensional eggbox-type charge modulation with \mathbf{q}_c oriented along the vertical directions can account for the basic Fermi surface (FS) features in the optimally and underdoped Bi2212 compounds. Here we supplement these considerations by a detailed analysis of the photoemission lineshape in the superconducting state. Concerning the frequency dependent part of the susceptibility we restrict ourselves to the simplest case of a single energy excitation, i.e. we choose $g(\nu) = \delta(\nu - \omega_0)$.

In Fig. 1 we show the spectral function at $(\pi, 0)$ and the $\Gamma \rightarrow X$ FS crossing in comparison with experimental data from Ref. [15]. Following the procedure in Ref. [15] we have added a step-like function to the spectra in order to incorporate the background.

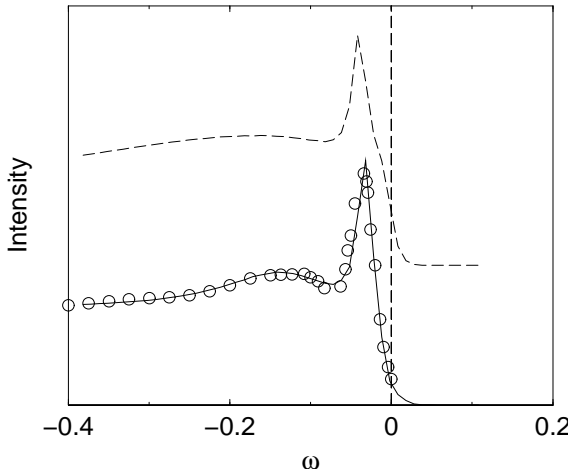


FIG. 1. Spectral function at $(\pi, 0)$ (solid line) and at $(0.35\pi, 0.35\pi)$ (dashed line). The experimental data points are taken from Ref. [15]. Parameters: $\omega_0 = 70\text{meV}$, $\lambda = 50\text{meV}$, $\Gamma = 0.5$, $|q_c| = \pi/3$.

Note that within our approximation of a single energy excitation a given state (\mathbf{k}, ω) is coupled via the CDW fluctuations to $(\mathbf{k} + \mathbf{q}, \omega - \omega_0)$ weighted by the charge-charge correlation function $J(\mathbf{q})$. As a consequence the structure of the hump feature is mainly determined by $J(\mathbf{q})$. From our fit to the experimental data we can therefore deduce that in Bi2212 the underlying CDW fluctuations are rather short-ranged i.e. the stripe correlations extend over 2-3 unit cells only. Moreover, due to the flatness of the bare bandstructure near the M-points the CDW fluctuations are most effective in these regions of \mathbf{k} -space as can be seen in Fig. 1. In contrast electronic states along the $\Gamma \rightarrow X$ direction can only scatter to rather high energies therefore leading to a significant reduction of the hump feature. Thus both antiferromagnetic (AF) and incommensurate CDW fluctuations have similar effects on the electronic self-energy and it is worth speculating that they coexist and work cooperatively in determining the physics of underdoped high- T_c superconductors.

B. $\text{La}_{2-x}\text{Sr}_x\text{CuO}_4$

In underdoped $\text{La}_{2-x}\text{Sr}_x\text{CuO}_4$ the incommensurate magnetic fluctuations display a four-fold pattern around (π, π) . For the Nd-doped lanthanum cuprate it has been argued [23] that this may be related to 2 types of twin domains, each with a single stripe orientation, since a two-dimensional pattern would not be consistent with the LTT symmetry of the system. However, this kind of argument no longer holds in case of underdoped LSCO where both the (tetragonal) a- and b- axes are at about 45° with respect to the CuO_6 tilt direction. Moreover it has been demonstrated in Refs. [24,25] that the posi-

tions of the elastic magnetic peaks in $\text{La}_{1.88}\text{Sr}_{0.12}\text{CuO}_4$ and excess-oxygen doped $\text{La}_2\text{CuO}_{4+y}$ are shifted off of the high-symmetry Cu-O-Cu directions by a tilt angle of $\Theta \approx 3^\circ$. For a one-dimensional stripe model this would correspond to one kink every ~ 19 Cu sites on the charge domain wall. However, as explicitly stated in Ref. [25] a grid pattern of orthogonal stripes oriented along the two orthorombic directions adequately describes the data as well.

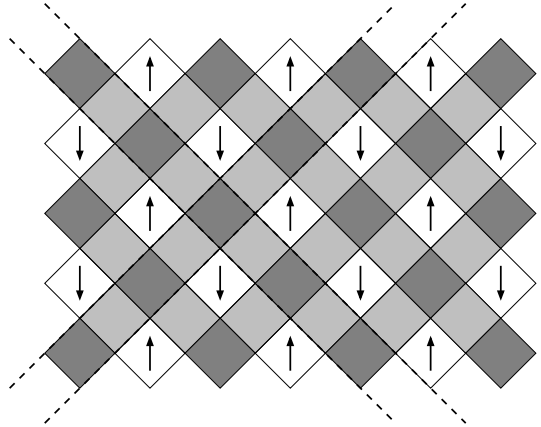


FIG. 2. Sketch of the two-dimensional charge- and spin modulation which is consistent with the AF peak incommensurability of LSCO. The pattern can be constructed from charge stripes running along the diagonal directions as indicated by the dashed lines. The crossing of two stripes leads to regions with high charge density (dark squares) whereas the residual segments of the stripes have intermediate charge (lightly shaded squares). The white squares illustrate the charge depleted areas with maximal spin density while the arrows indicate the sign of the AF order parameter.

In the following we therefore examine the consequences of this kind of two-dimensional dynamic stripe fluctuations on the electronic structure of LSCO and compare with photoemission experiments. Denoting the two orthogonal charge scattering vectors (which for simplicity we assume to have equal magnitude) by $\mathbf{q}_c^\pm = q_c(1, \pm 1)$ the charge modulation can be written as $\rho(\mathbf{R}) \sim \cos(q_c x) \cos(q_c y)$. Fig. 2 shows a sketch of the corresponding charge pattern which can be thought of an array of stripes running along the $(1, 1)$ and $(1, -1)$ directions respectively. Although our calculations are restricted on the charge channel we want to note that the corresponding pattern of the topological spin order can be constructed by assuming a sign change of the AF order parameter upon crossing the stripes perpendicular to their orientation. Thus the spin order follows the relation $\Delta^{spin}(\mathbf{R}) \sim \cos[q_c(x + y)/2] \cos[q_c(x - y)/2] \sim \cos(\mathbf{q}_s^+ \cdot \mathbf{R}) + \cos(\mathbf{q}_s^- \cdot \mathbf{R})$ where the spin scattering vectors are given by $\mathbf{q}_s^+ = q_c(1, 0)$ and $\mathbf{q}_s^- = q_c(0, 1)$ respectively. Thus this kind of two-dimensional scattering displays a deviation between charge- and spin direction of 45° where

the latter is compatible with the results of neutron scattering experiments [7,8]. Only in case of a LTT distortion both charge- and spin scattering collapse into a single direction leading to a reduction of T_c [6].

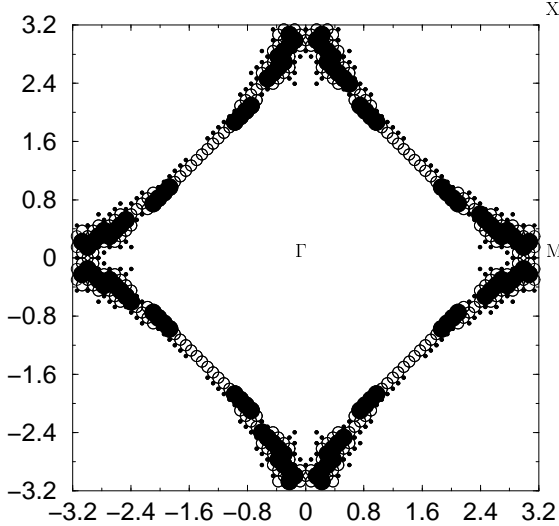


FIG. 3. Fermi surface for a system with two-dimensional diagonal CDW modulation ($q_c = \pi/5, \lambda = 0.01$). The plot is for temperature $T = 100K$ and the energy window around E_F has choosen to be 30meV. Intensities: $I > 50\%$: full points, $10\% < I < 50\%$: circles, $1\% < I < 10\%$: small dots.

As in the case of Bi2212 we restrict in the following on the charge channel and as discussed above we consider scattering along the $\mathbf{q}_c^\pm = (1, \pm 1)$ directions. To gain some qualitative insight we consider first the static non-superconducting case inspired by the approach described in Ref. [19] where we have derived an effective interaction $\frac{1}{2N} \sum_q V_q \rho_q \rho_{-q}$ for charge carriers close to an incommensurate CDW instability. Upon factorizing the interaction the two-dimensional eggbox-type charge modulation can be implemented by $\langle \rho_q \rangle^{egg} = \langle \rho_q \rangle [\delta_{q,q_c^+} + \delta_{q,q_c^-}]$ which in the static limit identifies the coupling parameter λ with the order parameter of the CDW $V(\mathbf{q}_c) \langle \rho_{\mathbf{q}_c} \rangle$. The resulting one particle hamiltonian can now be diagonalized and as a result we show in Fig. 3 the Fermi surface for an eggbox-type charge modulation with scattering vectors $\mathbf{q}_c = \pi/5(1, \pm 1)$.

Obviously diagonal CDW scattering strongly reduces the spectral intensity of the Fermi surface along the $\Gamma \rightarrow X$ direction. This is connected with the fact that along the diagonals the scattering vector is parallel to the contours of the bare bandstructure. As a consequence the CDW scattering is most efficient in these regions since \mathbf{q}_c can connect states with equal energies leading to a redistribution of spectral weight near $(\pi/2, \pi/2)$. Note that since the band disperses rather rapidly along $\Gamma \rightarrow X$ the vertical scattering we have adopted in case of Bi2212 leaves the electronic structure in this direction nearly unchanged.

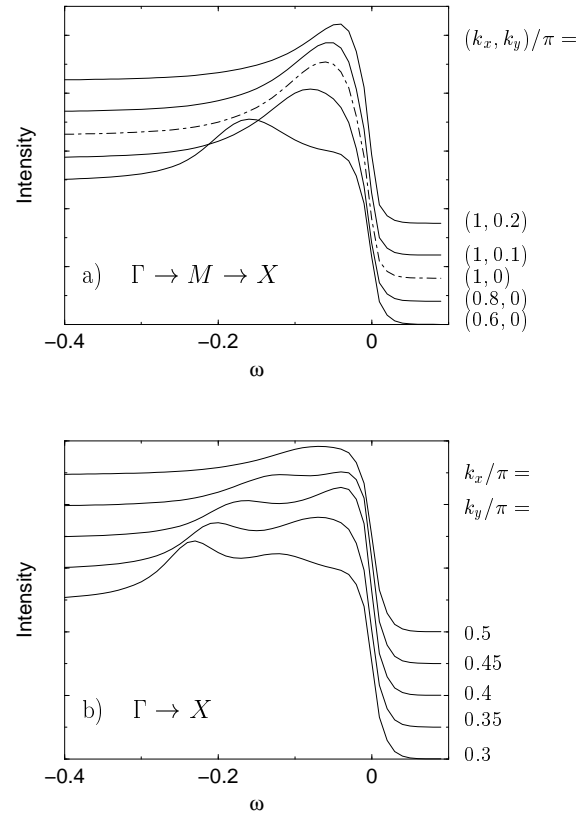


FIG. 4. Photoemission spectra for diagonal two-dimensional CDW scattering. As in the case of Bi2212 we have added a step-like function in order to model the background contribution. Parameter: $\omega_0 = 30\text{meV}$, $\Gamma = 0.01$, $\mathbf{q}_c = \pi/5(1, \pm 1)$.

Let us now extend the photoemission lineshape analysis to the superconducting state including dynamic incommensurate CDW scattering. We have found that for the LSCO compound a linear frequency distribution $g(\nu) = \frac{2\nu}{\omega_0^2} \Theta(\omega_0 - \nu)$ up to a cutoff energy ω_0 is more appropriate consistent with the experimental observation of low energy magnetic fluctuations in this compound. Fig. 4 shows selected energy distribution curves along $\Gamma \rightarrow M \rightarrow X$ (Fig. 4a) and $\Gamma \rightarrow X$ (Fig. 4b).

Note that we have used a rather large charge-charge correlation length (~ 100 lattice constants) in order to effectively suppress the quasiparticle peak along $(0, 0) \rightarrow (\pi, \pi)$. In this direction (Fig. 4b) one observes only a broad and weak incoherent feature which disappears beyond $k_x = k_y \sim 0.45\pi$ corresponding to the FS crossing of the underlying bare bandstructure. In contrast the spectra around $(\pi, 0)$ (Fig. 4a) are composed of an also broadened but still well pronounced quasiparticle peak. Due to the small cutoff energy ω_0 in comparison with Bi2212 and the additional linear frequency distribution the hump feature is no longer separated from the sharp peak but both collapse into the broadened peak shown in Fig. 4b.

IV. CONCLUSION

We have demonstrated that the coupling of a superconducting system to dynamical incommensurate CDW fluctuations can account for the observed ARPES photoemission lineshapes in both Bi2212 and LSCO materials. According to our analysis the vertically oriented CDW fluctuations in Bi2212 are rather fast and short ranged leading to the experimentally observed dip-hump structure around the M-points whereas the lineshape along the diagonals is hardly affected by the scattering. We note that in a recent preprint [26] Eschrig and Norman have analyzed ARPES data within a model of electrons interacting with a magnetic resonance using a similar approach than in the present paper. As already discussed above it is obvious that both AF- and CDW scattering have similar effects on the electronic states around the M-points (the renormalization function $Z(\omega)$ obtained from our approach is quasi identical to Fig. 1 in Ref. [26]). In this sense our work is not in contrast with Ref. [26] but rather complementary since the stripe fluctuations we consider here are anharmonic CDW's with the strong correlation playing a relevant role in the hole-poor regions, where antiferromagnetism is quite pronounced.

In case of LSCO the photoemission data can be described by a two-dimensional, diagonally oriented CDW which is slowly fluctuating and characterized by a rather large correlation length. This is consistent with the idea of long-range AF order coexisting with superconductivity in the 214 systems and also with the more pronounced tendency to form static charge textures in these materials. We have shown that within this scenario the QP along the $(0, 0) \rightarrow (\pi, \pi)$ direction can be effectively suppressed whereas around the M-points a broad quasiparticle peak persists. Finally we want to emphasize that since Δ_{SC} enters the calculation as an input parameter, our model does not include the phase fluctuations of the particle-particle pairs. These fluctuations should play a major role in destroying the quasiparticle peak above T_c [27]. However, the measurements by Ino et al. [17] on LSCO were done at rather low temperatures ($T=15\text{K}$) where such phase fluctuations are ineffective justifying our simplified model for the photoemission spectra.

ACKNOWLEDGMENTS

We greatly acknowledge useful discussions with S. Caprara, C. di Castro and C. Castellani.

[1] S. Sachdev and J. Ye, Phys. Rev. Lett. **69**, 2411 (1992).

- [2] C. M. Varma, Phys. Rev. Lett. **75**, 898 (1995).
- [3] C. Castellani, C. Di Castro, and M. Grilli, Phys. Rev. Lett. **75**, 4650 (1995); C. Castellani, C. Di Castro, and M. Grilli, Z. für Physik, **103**, 137 (1997).
- [4] A. Perali, C. Castellani, C. Di Castro, and M. Grilli, Phys. Rev. B **54**, 16216 (1996).
- [5] C. Castellani, C. Di Castro, and M. Grilli, J. Phys. Chem. Solids **59**, 1694 (1998).
- [6] J. M. Tranquada, B. J. Sternlieb, J. D. Axe, Y. Nakamura, and S. Uchida, Nature **375**, 561 (1995).
- [7] K. Yamada, C. H. Lee, K. Kurahashi, J. Wada, S. Wakimoto, S. Ueki, H. Kimura, Y. Endoh, S. Hosoya, G. Shirane, R. J. Birgeneau, M. Greven, M. A. Kastner, and Y. J. Kim, Phys. Rev. B **57**, 6165 (1998).
- [8] M. Arai, T. Nishijima, Y. Endoh, T. Egami, S. Tajima, K. Tomimoto, Y. Shiohara, M. Takahashi, A. Garrett, S. Bennington, Phys. Rev. Lett. **83**, 608 (1999).
- [9] G. B. Teitelbaum, B. Büchner, H. de Gronckel, cond-mat/0005090.
- [10] S. Krämer, M. Mehring, Phys. Rev. Lett. **83**, 396 (1999).
- [11] A. W. Hunt, P. M. Singer, K. R. Thurber, and T. Imai, Phys. Rev. Lett. **82**, 4300 (1999).
- [12] J. L. Tallon, J. W. Loram, G. V. Williams, J. R. Cooper, I. R. Fisher, J. D. Johnson, M. P. Staines, C. Bernhard, Phys. Stat. Sol. B, 215, 531 (1999).
- [13] G. S. Boebinger, Yoichi Ando, A. Passner, T. Kimura, M. Okuya, J. Shimoyama, K. Kishio, K. Tamasaku, N. Ichikawa, S. Uchida, Phys. Rev. Lett. **77**, 5417 (1996).
- [14] M. R. Norman, H. Ding, J. C. Campuzano, T. Takeuchi, M. Randeria, T. Yokoya, T. Takahashi, T. Mochiku, and K. Kadowaki, Phys. Rev. Lett. **79**, 3506 (1997).
- [15] M. R. Norman and H. Ding, Phys. Rev. B **57**, R11089 (1998).
- [16] J. C. Campuzano, H. Ding, M. R. Norman, H. M. Fretwell, M. Randeria, A. Kaminski, J. Mesot, T. Takeuchi, T. Sato, T. Yokoya, T. Takahashi, T. Mochiku, K. Kadowaki, P. Guptasarma, D. G. Hinks, Z. Konstantinovic, Z. Z. Li, and H. Raffy, Phys. Rev. Lett. **83**, 3709 (1999).
- [17] A. Ino, C. Kim, M. Nakamura, T. Yoshida, T. Mizokawa, Z.-X. Shen, A. Fujimori, T. Kakeshita, H. Eisaki, and S. Uchida, Phys. Rev. B **62**, 4137 (2000).
- [18] T. Tohyama, S. Nagai, Y. Shibata, and S. Maekawa, Phys. Rev. Lett. **82**, 4910 (1999).
- [19] G. Seibold, F. Becca, F. Bucci, C. Castellani, C. Di Castro, and M. Grilli, Europ. Phys. J. B **13**, 87 (2000).
- [20] A. P. Kampf and J. R. Schrieffer, Phys. Rev. B **42**, 7967 (1990).
- [21] M. R. Norman, Phys. Rev. B **61**, 16117 (2000).
- [22] C. Kim, P. J. White, Z.-X. Shen, T. Tohyama, Y. Shibata, S. Maekawa, B. O. Wells, Y. J. Kim, R. J. Birgeneau, and M. A. Kastner, Phys. Rev. Lett. B **80**, 4245 (1998).
- [23] J. M. Tranquada, Physica B **241-243**, (1998).
- [24] Y. S. Lee, R. J. Birgeneau, M. A. Kastner, Y. Endoh, S. Wakimoto, K. Yamada, R. W. Erwin, S.-H. Lee, and G. Shirane, Phys. Rev. B **60**, 3643 (1999).
- [25] H. Kimura, H. Matsushita, K. Hirota, Y. Endoh, K. Yamada, G. Shirane, Y. S. Lee, M. A. Kastner, and R. J. Birgeneau, Phys. Rev. B **61**, 14366 (2000).
- [26] M. Eschrig and M. R. Norman, cond-mat/005390.
- [27] M. Franz and A. J. Millis, Phys. Rev. B **58**, 14572 (1998).